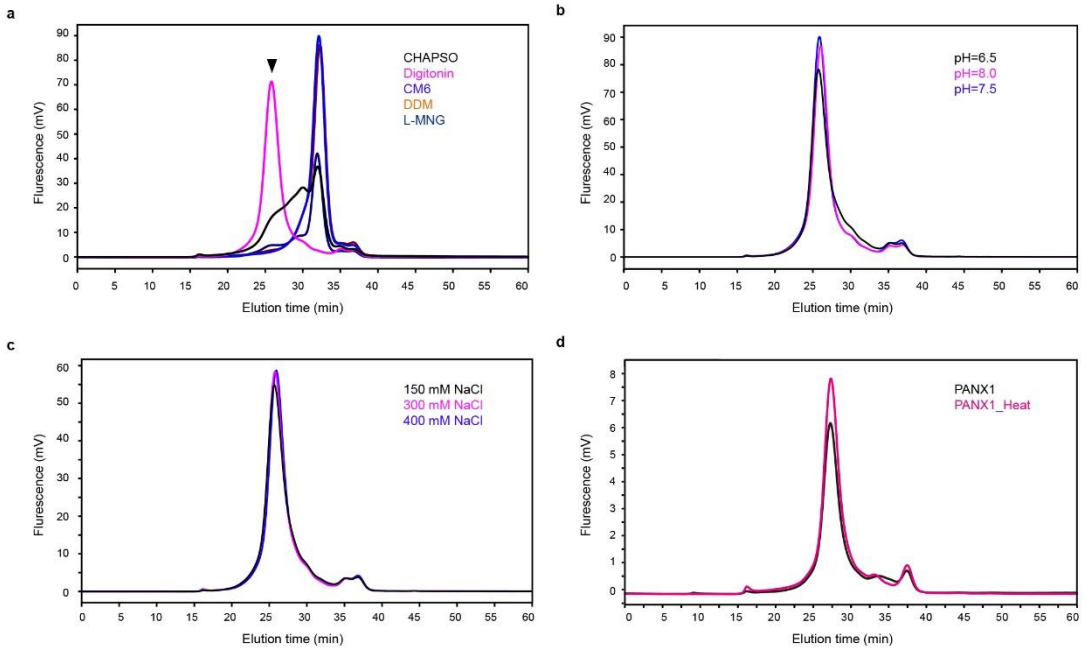

Supplementary information, Fig. S1 Screening purification conditions for PANX1 channel protein. (a-c) FSEC screening of detergent (a), pH (b), and salt (c) conditions for PANX1 protein purification. The black triangle in (a) marks the polymeric assembly of the PANX1 channel. CM6 represents 6-cyclohexyl-1-hexyl-β-D-maltoside, DDM represents n-dodecyl β-D-maltoside, and L-MNG represents L-maltose-neopentyl glycol. (d) Thermostability test of PANX1 protein solubilized from HEK293S GnTI^{-} cells with digitonin.

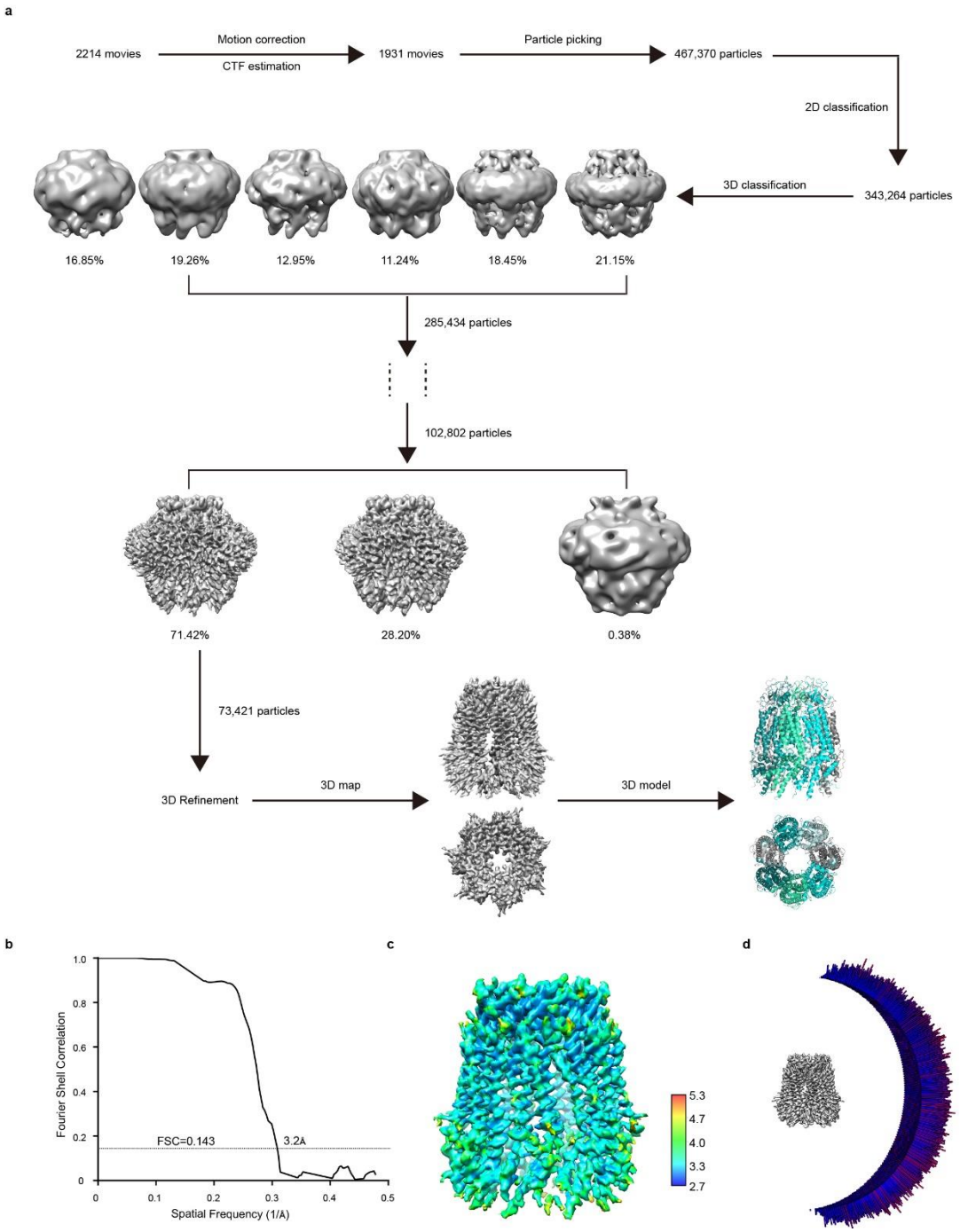

Supplementary information, Fig. S2 Overview of cryo-EM image processing and 3D reconstruction. (a) Flowchart of the image processing and model building of the PANX1 channel. (b) Fourier shell correlation (FSC) curve for the resolution estimation. (c) Side view of the cryo-EM density map colored by local resolution estimated by ResMap. (d) Euler angle distribution of the particles used for the 3D reconstruction.

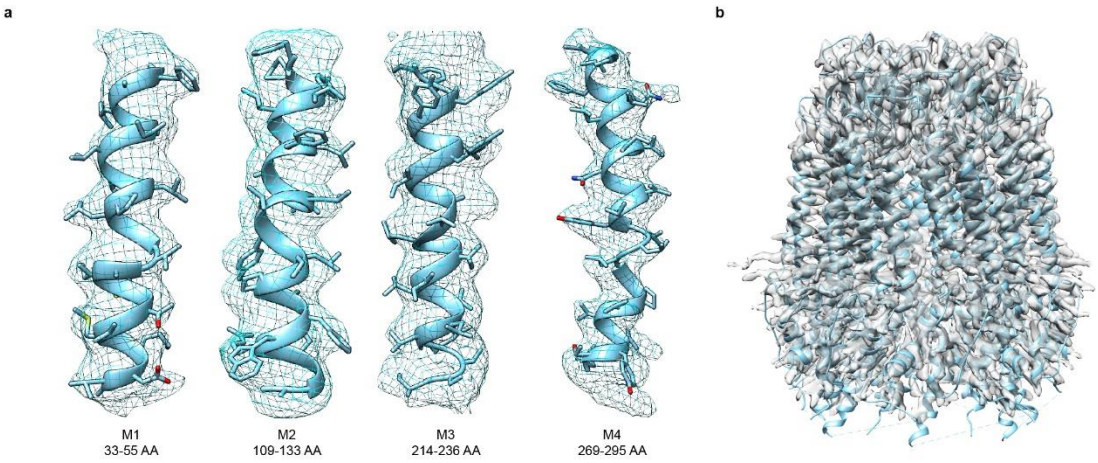

Supplementary information, Fig. S3 The PANX1 atomic model fit to the cryo-EM density map. (a) The segmented cryo-EM map (blue mesh) with the atomic model is shown as sticks and ribbons, and the transmembrane helices M1–M4 are identified, which are the most well-defined. (b) The ribbon style model of the PANX1 channel fit to the 3.2 Å density map.

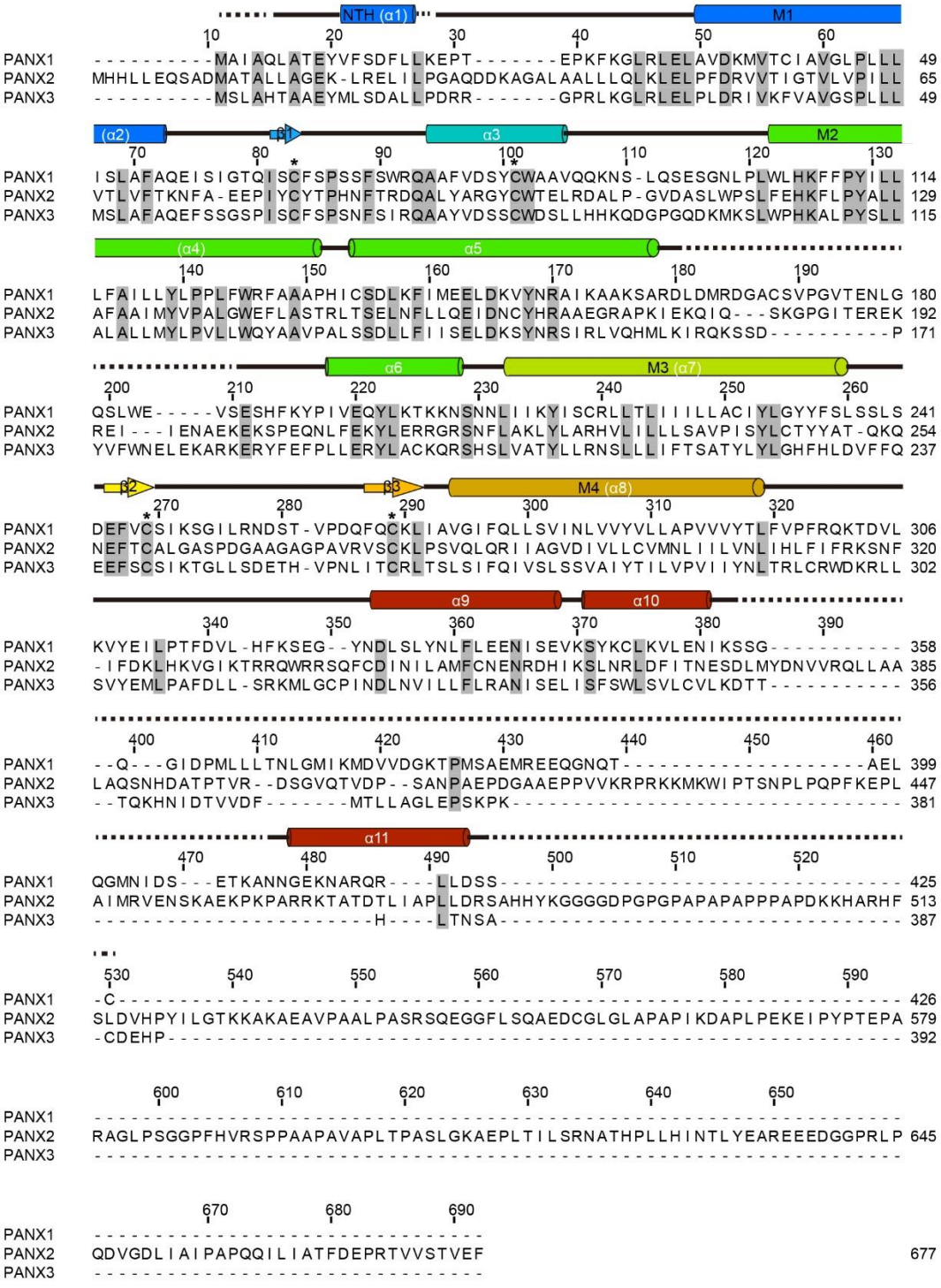

Supplementary information, Fig. S4 Sequence alignment of the Pannexin family. Human PANX1, PANX2, and PANX3 were aligned according to their amino acid sequences by ClustalW. Cartoon representations of the secondary structure elements of PANX1 with the same colors as in Fig. 1f are shown above the sequences. Cylinders represent α-helices, arrows represent β-sheets, lines represent loops, and dashed lines represent the sequences unfitted on the map. Gray shading shows the 100% conserved residues, and the conserved four extracellular cysteines are marked with asterisks.

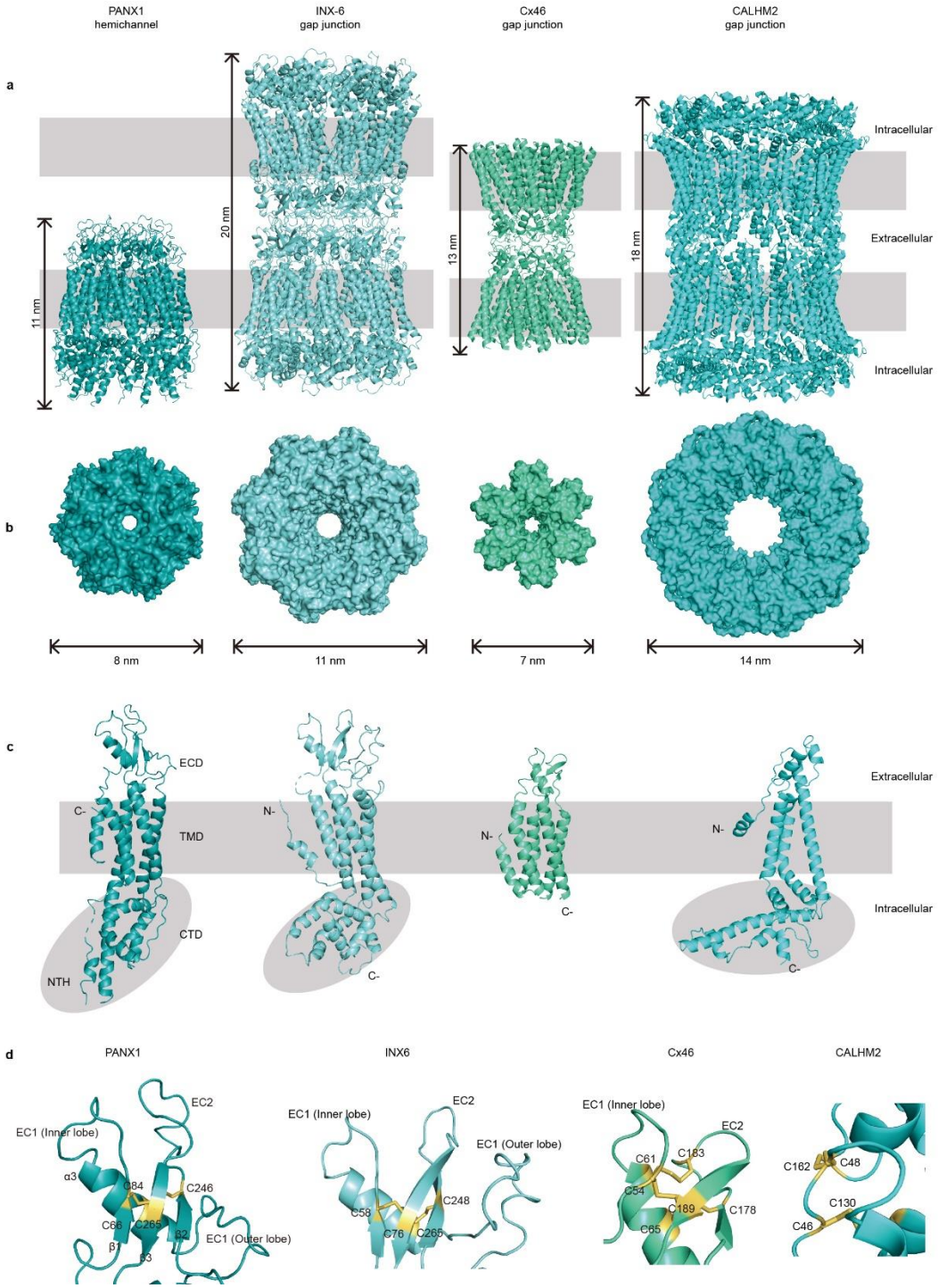

Supplementary information, Fig. S5 Structural comparisons of PANX1, INX-6, Cx46, and CALHM2 channels. (a-b) The side-views of cartoon (a) and top-views of surface (b) representations of PANX1, INX-6 (PDB code: 5H1R),[12] Cx46 (PDB code: 6MHQ),[13] and CALHM2 (PDB code: 6UIX)[14] channels are presented. The lengths and widths of each channel and regions corresponding to the extracellular, transmembrane, and cytoplasmic regions are indicated. (c) The protomer structures of the PANX1, INX-6, Cx46, and CALHM2 channels with the N- and C-termini marked. (d) The distributions of the disulfide bonds in the extracellular domain (ECD). The corresponding secondary elements are indicated, and disulfide bonds are labeled in yellow sticks.

Table S1 Cryo-EM data collection, refinement, and validation statistics

	PANX1
Data collection and processing	
Magnification	81,000
Voltage (kV)	300
Electron exposure ($e^-/Å^2$)	67
Defocus range (μm)	−1.5 to −3
Pixel size (Å)	1.045
Symmetry imposed	C7
Initial particle images (no.)	467,370
Final particle images (no.)	73,421
Map resolution (Å)	3.2
Map-sharpening B-factor ($Å^2$)	−103
Refinement	
R.m.s deviations	
Bond lengths (Å)	0.007
Bond angles (°)	0.932
Ramachandran plot	
Favored (%)	94.41
Allowed (%)	5.59
Outliers (%)	0

Supplementary information

Materials and Methods

Construct design and FSEC screen

Human *PANX1* coding sequence (NM_015368.4, residues 1–426, GenBank: NP_056183) was cloned into the pEG BacMam vector, followed by a 3C protease cleavage site, an enhanced red fluorescent protein mRuby, and a Step II affinity tag. Wild-type human PANX1 was expressed in HEK293S GnTI^{-} cells using Polyethylenimine (PEI) transfection. At 8 hours post-transfection, the medium was replaced with DMEM supplemented with 10 mM sodium butyrate. Cells were collected at 36 hours with cold TBS buffer (150 mM NaCl, 20 mM Tris-HCL at pH 8.0) and centrifuged at 4,000 × *g* for 5 min at 4°C. Cells were resuspended in the solubilization buffer containing 150 mM NaCl, 20 mM Tris-HCL pH 8.0, 1% digitonin, and protease inhibitor cocktail (2 mg/mL leupeptin, 2 mM pepstatin A, 0.8 mM aprotinin, and 1 mM phenylmethylsulfonyl fluoride). For the pH test the buffer was changed to 20 mM MES at pH 6.5 or HEPES at pH 7.0, for the salt concentration test the NaCl concentration was changed to 300 mM or 400 mM, and for the detergent test digitonin was changed to CHAPSO, 6-cyclohexyl-1-hexyl-β-D-maltoside, n-dodecyl β-D-maltoside, or L-maltose-neopentyl glycol. Samples were rotated at 4°C for 1 hour and then ultra-centrifuged at 40,000 × *g* for 40 min at 4°C. The supernatants were analyzed by fluorescence-detection size-exclusion chromatography (FSEC) to screen the purification conditions. To test the thermostability of PANX1 protein, the samples were

split into two equal parts. One part was heated at 50°C for 10 min and then analyzed by FSEC after ultra-centrifugation.

Protein expression and grid preparation

Baculovirus containing PANX1 were generated according to the Bac-to-Bac system protocol (Invitrogen). P2 viruses were used to infect a suspension of HEK293 GnTI^{-} cells at a density of 3.0×10^6 cells/mL. At 12 hours post-infection, 10 mM sodium butyrate was added to the culture medium and the temperature was shifted to 30°C. Cells were collected 60 hours post-infection and subsequently sonicated in TBS buffer supplemented with protease inhibitor cocktail. The homogenate was centrifuged at 8,000 × *g* for 20 min at 4°C to remove the cell debris. The supernatant was further ultra-centrifuged at 40,000 × *g* for 1 hour at 4°C to enrich the membrane fraction. The membrane pellet was then solubilized with solubilization buffer for 1.5 hour at 4°C. Non-solubilized material was removed by ultracentrifugation (40,000 × *g*, 4°C for 1 hour), and the soluble fraction was bound to the Strep-tactin beads and eluted with TBS buffer supplemented with 0.25% digitonin and 5 mM desthiobiotin. After 3C protease digestion overnight at 4°C, the PANX1 protein was further purified by size-exclusion chromatography (SEC) using a Superose 6 10/300 GL column equilibrated with buffer consisting of 150 mM NaCl, 0.1% digitonin, and 20 mM Tris-HCl at pH 8.0.

Peak fractions collected from SEC were concentrated to 3.5–4.0 mg/mL and then ultra-centrifuged at 40,000 × *g* for 1 hour at 4°C. A total of a 3 μL sample was applied to a glow-discharged Quantifoil holey carbon grid (gold, 1.2–1.3 μm/hole, 200 mesh),

blotted using a Vitrobot (FEI) with a 3 s blotting time at 100% humidity and 18°C, and then plunge-frozen in liquid ethane cooled by liquid nitrogen. The frozen grids were carefully transferred and stored in liquid nitrogen until Cryo-EM image collection.

Data collection and image processing

A total of 2,214 movies were collected on a Titan Krios (FEI) operated at 300 kV equipped with a Gatan image filter (operated with a slit width of 20 eV) (GIF), mounted with a K3 Summit detector (Gatan, Inc.). SerialEM[1] was used to automatically acquire micrographs in super-resolution counting mode at a pixel size of 0.5225 Å and with nominal defocus values ranging from −1.5 to −3 μm. Movies with 36 frames each were collected at a dose of 25 electrons per pixel per second over an exposure time of 3 s, resulting in a total dose of 67 $e^{-}/Å^2$ on the specimen.

All 36 movie frames in each stack were aligned and dose weighted using MotionCor2,[2] which generated 2-fold binned images to a pixel size of 1.045 Å/pixel. CTFFIND 4.1[3] was used for estimating the defocus values and astigmatism parameters of the contrast transfer function (CTF). A total of 1931 micrographs were chosen for further processing. cisTEM[4] was initially used for image processing. In order to get an idea of the subunit organization, reference-free two-dimensional (2D) classifications were performed. RELION 3.0 was used for further data processing.

About 3,000 particles were initially picked by ManualPick from selected micrographs and subjected to 2D classification. The reference-free 2D class averages selected from manually picking particles were used as templates for automated particle picking,

which yielded a total of 467,370 particles. These particles were extracted with a box size of 320 × 320 pixels and processed with rounds of iterative 2D and 3D classifications. 3D classification was performed using an initial model generated *de novo* from 2D particles by using the stochastic gradient descent (SGD) algorithm, low-pass filtered to 30 Å. In the 2D class averages or 3D class reconstructions, those particles without high-resolution and interpretable features were considered as "bad class" and were discarded. C7 symmetry was applied, which was first compared with C1 and showed better map features. Finally, 73,421 particles from a 3D class showing good secondary structural features in the transmembrane domain were selected for further 3D refinement. Post-processing yielded a map with an overall resolution of 3.2 Å according to the Fourier shell correlation (FSC) equal to 0.143 criterion.[5] The local resolution was calculated by ResMap.[6] The masks used for the FSC calculations were produced using relion_mask_create in RELION 3.0.

Model building and refinement

The PANX1 protein structure was modeled *de novo*. Much of the side-chain density information was clearly visualized in the map, which made the unambiguous building and refining of the model possible. Coot was used to build the atomic model,[7] which was then refined via the real_space_refinement feature in Phenix.[8] Pore radii were measured by the program HOLE.[9] All of the figures were created using USCF Chimera[10] or PyMOL 2.3.2.

Sequence analysis and alignment of the Pannexin family

Homologous sequences of the human Pannexin family (PANX1, PANX2 and PANX3) were aligned by ClustalW (https://www.ebi.ac.uk/Tools/msa/clustalw2/) and displayed using Adobe Illustrator.

Mouse oocyte collection, cRNA transcription, and microinjection

GV oocytes were acquired from 6–8-week-old female ICR mice (Beijing Vital River Laboratory Animal Technology Co.) by puncturing the antral follicles with a fine needle under a dissecting microscope. GV oocytes were cultured in M2 medium (Sigma-Aldrich) supplemented with 10% FBS.

The full-length of human *PANX1* gene coding sequence following a stop codon (NM_015368.4) was amplified and cloned into the pCMV6-entry vector to express an untagged protein. The p.W74A mutation in *PANX1* was introduced by using the KOD-Plus-Mutagenesis Kit (Toyobo Life Science) following the manufacturer's instructions. WT and mutant PANX1 were linearized by *AgeI* restriction enzyme (R0552S, New England Biolabs) for 3 hours at 37 °C. A total of 1 μg purified linearized DNA was used as a template to transcribe the cRNA of *PANX1* using the HiScribe T7 ARCA mRNA Kit (E2060S, New England BioLabs), followed by DNase I treatment and polyadenylate tailing, and the cRNA was further purified using the RNeasy MinElute Cleanup Kit (74204, Qiagen).

About 5–10 pL (1000 ng/mL) of WT or mutant *PANX1* cRNA was microinjected into the cytoplasm of GV oocytes using a Leica Hoffman microscope (LSM6000) equipped

with a TransferMan NK2 micromanipulator and InjectMan NI2 (Eppendorf). The injected GV oocytes were matured in M2 medium (Sigma-Aldrich) supplemented with 10% FBS for 12 hours at 37°C with 5% CO_2. Mature oocytes were gathered and fertilized with capacitated sperm. All mouse experimental protocols were ethically reviewed by the Shanghai Medical College of Fudan University.

Two-electrode voltage-clamp recording

A total of 6 ng of WT or mutant *PANX1* cRNA was injected into *Xenopus laevis* oocytes. Two-electrode voltage-clamp (TEVC) was performed 48 hours later in the standard external solution that included 2 mM $CaCl_2$, 2 mM KCl, 1 mM $MgCl_2$, 90 mM NaCl, and 5 mM HEPES with or without 10 mM CBX (Sigma-Aldrich). The pH was adjusted with KOH to 7.4. Initially, the membrane potential was held at −60 mV for 100 ms, then changed from −100 to +60 mV in 2 s ramps with 20 mV per step. Data were gathered and analyzed using a pClamp10 (Molecular Devices). Statistical analyses were carried in GraphPad Prism, and data are shown as means ± SD with a *p*-value blow 0.05 being considered significant.

ATP release measurements

HEK293S GnTI$^-$ cells were plated in 24-well plates and transfected with WT or mutant PANX1 plasmid at 80–90% confluence. The measurement of ATP release was conducted using an ATP Bioluminescent Assay Kit (Sigma-Aldrich) according to the manual and the method that Lohman et al. used in 2012.[11] Briefly, 30–36 hours after

transfection, the medium was removed from each well and fresh medium was added. A total volume of 300 μM ARL 67156 (Sigma-Aldrich) was added for 30 min at 37°C to inhibit the ectonucleotidases. HEK293S GnTI^{-} cells were stimulated by 100 mM KCl for 1 min, and following stimulation of the cells 100 μL of the supernatant was collected and immediately placed on ice. All samples were then centrifuged at 5000 × *g* for 2 min and transferred to a new tube. A mixture of 50 μL of each sample and 50 μL of luciferin-luciferase was assayed using a luminometer (Luminoskan TL Plus, Thermo LabSystems). The relative ATP concentration was displayed as a ratio of all values with respect to the control group.

Statistical analysis

GraphPad was used to perform the statistical analyses. Student's *t*-tests and one-way ANOVA followed by Tukey's post-hoc test was used for two experimental groups and more than two groups, respectively. P-values less than 0.05 were considered significant.

References

1. Mastronarde, D. N., Automated electron microscope tomography using robust prediction of specimen movements. *J. Struct. Biol.* **152**, 36-51 (2005).

2. Zheng, S. Q. et al., MotionCor2: anisotropic correction of beam-induced motion for improved cryo-electron microscopy. *Nat. Methods* **14**, 331-332 (2017).

3. Rohou, A. & Grigorieff, N., CTFFIND4: Fast and accurate defocus estimation from electron micrographs. *J. Struct. Biol.* **192**, 216-221 (2015).

4. Grant, T., Rohou, A. & Grigorieff, N., cisTEM, user-friendly software for single-particle image processing. *Elife* **7**, (2018).

5. Henderson, R. et al., Outcome of the first electron microscopy validation task force meeting. *Structure* **20**, 205-214 (2012).

6. Kucukelbir, A., Sigworth, F. J. & Tagare, H. D., Quantifying the local resolution of cryo-EM density maps. *Nat. Methods* **11**, 63-65 (2014).

7. Emsley, P., Lohkamp, B., Scott, W. G. & Cowtan, K., Features and development of Coot. *Acta Crystallogr D Biol Crystallogr* **66**, 486-501 (2010).

8. Adams, P. D. et al., PHENIX: a comprehensive Python-based system for macromolecular structure solution. *Acta Crystallogr D Biol Crystallogr* **66**, 213-221 (2010).

9. Smart, O. S., Neduvelil, J. G., Wang, X., Wallace, B. A. & Sansom, M. S., HOLE: a program for the analysis of the pore dimensions of ion channel structural models. *J Mol Graph* **14**, 354-360, 376 (1996).

10. Pettersen, E. F. et al., UCSF Chimera--a visualization system for exploratory

research and analysis. *J. Comput. Chem.* **25**, 1605-1612 (2004).

11. Lohman, A. W. et al., S-nitrosylation inhibits pannexin 1 channel function. *J. Biol. Chem.* **287**, 39602-39612 (2012).

12. Oshima, A., Tani, K. & Fujiyoshi, Y., Atomic structure of the innexin-6 gap junction channel determined by cryo-EM. *Nat Commun* **7**, 13681 (2016).

13. Myers, J. B. et al., Structure of native lens connexin 46/50 intercellular channels by cryo-EM. *Nature* **564**, 372-377 (2018).

14. Choi, W., Clemente, N., Sun, W., Du J & Lu, W., The structures and gating mechanism of human calcium homeostasis modulator 2. *Nature* **576**, 163-167 (2019).